JGR Biogeosciences

RESEARCH ARTICLE
10.1029/2022JG007197

Key Points:

- A seasonal variable such as canopy chlorophyll content was useful to predict gross primary productivity with machine learning models
- A clockwise hysteretic pattern of sap flow to radiation is a good indicator of water-related stomatal closure
- The light use efficiency of green parts of a spruce forest was 4.0% with a standard deviation of 2.3% during the 2021 growing season

Supporting Information:

Supporting Information may be found in the online version of this article.

Correspondence to:

O. Reitz,
oliver.reitz@geo.rwth-aachen.de

Citation:

Reitz, O., Bogena, H., Neuwirth, B., Sanchez-Azofeifa, A., Graf, A., Bates, J., & Leuchner, M. (2023). Environmental drivers of gross primary productivity and light use efficiency of a temperate spruce forest. *Journal of Geophysical Research: Biogeosciences*, *128*, e2022JG007197. https://doi.org/10.1029/2022JG007197

Received 21 SEP 2022
Accepted 25 JAN 2023

Environmental Drivers of Gross Primary Productivity and Light Use Efficiency of a Temperate Spruce Forest

O. Reitz[1], H. Bogena[2], B. Neuwirth[3], A. Sanchez-Azofeifa[4], A. Graf[2], J. Bates[2], and M. Leuchner[1]

[1]Physical Geography and Climatology, Institute of Geography, RWTH Aachen University, Aachen, Germany, [2]Agrosphere Institute, IBG-3, Forschungszentrum Jülich GmbH, Jülich, Germany, [3]DeLaWi Tree-Ring Analyses, Windeck, Germany, [4]Earth and Atmospheric Sciences Department, Centre for Earth Observation Sciences (CEOS), Edmonton, AB, Canada

Abstract Various environmental variables drive gross primary productivity (GPP) and light use efficiency (LUE) of forest ecosystems. However, due to their intertwined nature and the complexity of measuring absorbed photosynthetically active radiation (APAR) of forest canopies, the assessment of LUE and the importance of its environmental drivers are difficult. Here, we present a unique combination of measurements during the 2021 growing season including eddy covariance derived GPP, sap flow, Sentinel-2 derived canopy chlorophyll content and in situ measured APAR. The importance of environmental variables for GPP models is quantified with state-of-the-art machine learning techniques. A special focus is put on photosynthesis-limiting conditions, which are identified by a comparison of GPP and sap flow hysteretic responses to Vapor pressure deficit (VPD) and APAR. Results demonstrate that (a) LUE of the canopy's green part was on average 4.0% ± 2.3%, (b) canopy chlorophyll content as a seasonal variable for photosynthetic capacity was important for GPP predictions, and (c) on days with high VPD, tree-scale sap flow and ecosystem-scale GPP both shift to a clockwise hysteretic response to APAR. We demonstrate that the onset of such a clockwise hysteretic pattern of sap flow to APAR is a good indicator of stomatal closure related to water-limiting conditions at the ecosystem-scale.

Plain Language Summary The efficiency by which a forest uses sunlight to perform photosynthesis is an important feature for climate and ecosystem modeling. However, the light that is actually captured by forests and is useable for photosynthesis is difficult to assess. Here, we show a sophisticated approach to estimate the light use efficiency of a spruce forest in Germany and analyze environmental influences on it and on photosynthesis. Our results indicate that about 4% of the light useable for photosynthesis was actually used by the forest during the 2021 growing season and that seasonal variations of chlorophyll in the canopy are a good indicator for carbon capture.

1. Introduction

The gross primary productivity (GPP) of terrestrial ecosystems, of which forests are the dominant factor (Pan et al., 2011), is a key element of the global carbon cycle (Canadell et al., 2021). The resulting biomass further is important for human demands of food, energy, and construction materials (Taye et al., 2021). The assimilation of atmospheric CO_2 via photosynthesis is primarily driven by photosynthetically active radiation (PAR), though it is also sensitive to intertwined environmental and physiological variables, such as temperature, water, and nutrient availability, or chlorophyll content of the canopy (Anav et al., 2015; Bao et al., 2022; Keenan et al., 2012).

The light use efficiency (LUE) concept was established by Monteith (1972) and describes how efficiently solar energy is converted to chemical energy. It can be expressed as the ratio of GPP to the absorbed PAR (APAR). Under optimal conditions, a linear relation between GPP and APAR is assumed (Monteith, 1972), and LUE models utilize this logic for estimating GPP based on APAR and sensitivity functions for environmental conditions limiting LUE (e.g., Horn & Schulz, 2011; Stocker et al., 2020; S. Wang et al., 2018). The shape of these functions representing the response of LUE to meteorological variables, however, varies widely between approaches (Bao et al., 2022). Although LUE models are widely used to predict GPP, such as for the MODIS GPP product (Running & Zhao, 2015), they rely on accurate APAR measurements. For most sites with GPP data, these are only available from remote sensing derived fraction of APAR (fAPAR) products (Garbulsky et al., 2010). For forest ecosystems, however, fAPAR differed among satellite products (Tao et al., 2015) and

deviated from in situ fAPAR measurements, especially for temperate coniferous forests (Putzenlechner, Castro, et al., 2019). On the other hand, in situ measurements of fAPAR are laborious, especially for forest canopies, because of the high spatiotemporal variability of their light transmissivity (Leuchner et al., 2011; Vesala et al., 2000), which requires a sophisticated network of PAR sensors to capture the variability of different flux terms (Putzenlechner, Marzahn, et al., 2019; Widlowski, 2010). Hence, few studies investigated environmental controls of LUE for forest ecosystems based on in situ APAR measurements (Goulden et al., 1997; Urban et al., 2012).

With climate change, a shift from energy-limited to water-limited conditions is expected for many terrestrial ecosystems (Denissen et al., 2022), making it important to accurately identify and distinguish those conditions. Vapor pressure deficit (VPD) was found to be a dominant control for stomatal conductance and, thus, for limiting photosynthesis (Castro et al., 2018; Katul et al., 2003). Sap flow sensors measure the transport of water through the xylem and in this way provide a continuous proxy of stomatal conductance (Ewers et al., 2007; Köstner et al., 1998; Steppe et al., 2015). Brinkmann et al. (2016) compared the sap flow response to drying conditions of different European tree species and showed that the sap flow of *Picea abies* was especially sensitive to limited water availability. Hence, despite being promising for analyzing limiting conditions of photosynthesis, as shown by the usefulness of sap flow to estimate GPP (Klein et al., 2016), a combination of sap flow and GPP measurements has rarely been performed to show that the tree-scale sap flow response is analogous to that of the ecosystem-scale GPP.

Furthermore, the ratio of available light in the red to light in the far-red domain (R/FR) is a measure of light quality (Ammer, 2003; Turnbull, 1991) and can adapt chlorophyll content, though a direct relation to CO_2 assimilation could not be found (Heraut-Bron et al., 2000). Besides meteorological drivers, canopy nitrogen and leaf mass per area were shown to be important to explain the variation in LUE across species and environments (Green et al., 2003), though both are rarely considered in LUE models. The canopy chlorophyll content (CCC) incorporates both of these measures and showed a stronger relationship to GPP than leaf area index (LAI) or leaf chlorophyll content (C_{ab}) alone (Croft et al., 2015). GPP seasonality of a soybean field was further dominated by CCC, while APAR and sun induced chlorophyll fluorescence peaked about 2 weeks earlier (Wu et al., 2022). In view of such a plethora of environmental controls on GPP, variable importance measures of machine-learning models are a valuable tool to quantify the model importance of individual highly non-linear sensitivities that are otherwise difficult to quantify (Archer & Kimes, 2008; Grömping, 2009; Williamson et al., 2021).

For this study, a multitude of environmental data were collected for a European spruce forest, including eddy covariance derived GPP, APAR from a network of PAR sensors, sap flow of three trees, and various environmental variables including satellite derived CCC. Based on these data, our goals were threefold, to (a) assess the LUE of a spruce forest and analyze the impact of various environmental drivers on it, (b) quantify the importance of single environmental variables for machine-learning GPP models, and (c) identify limiting conditions of photosynthesis by linking tree-scale sap flow measurements to ecosystem-scale GPP and meteorological data.

2. Materials and Methods

2.1. Study Area Description

Measurements took place between 28 April and 30 September 2021 at the Wüstebach forest site (50°30′16″N, 6°19′50″E), Germany, which is part of the TERrestrial ENvironmental Observatories (TERENO) network (Bogena et al., 2018). The forest lies at 600–620 m asl within the Eifel National Park near the Belgian border and is a spruce monoculture (*Picea abies* (L.) H. Karst.) planted in 1946 with an overall tree density of 370 trees/ha (Etmann, 2009) and an average canopy height of 25 m. The understory mostly consisted of young beech plantings (*Fagus sylvatica* L.), *Vaccinium myrtillus* L., ferns (e.g., *Struthiopteris spicant* (L.) Roth) and various mosses. The dominant soil types are Cambisols and Planosols (Graf et al., 2014) and the dominant soil textures are silt loam and silty clay loam (Borchardt, 2012). During April–September 2021 the site had a mean temperature of 12.2°C, and received 629 mm of precipitation. At the nearest long-term official weather station Kall-Sistig of the German Weather Service, about 13 km to the east, this period was 0.6°C colder and had 158% of the precipitation compared to the 1991–2020 averages. April and May were especially cold (−3.2°C and −2.4°C deviation, respectively) and July was especially wet (347% of average), while June was significantly warmer than average (+2.4°C).

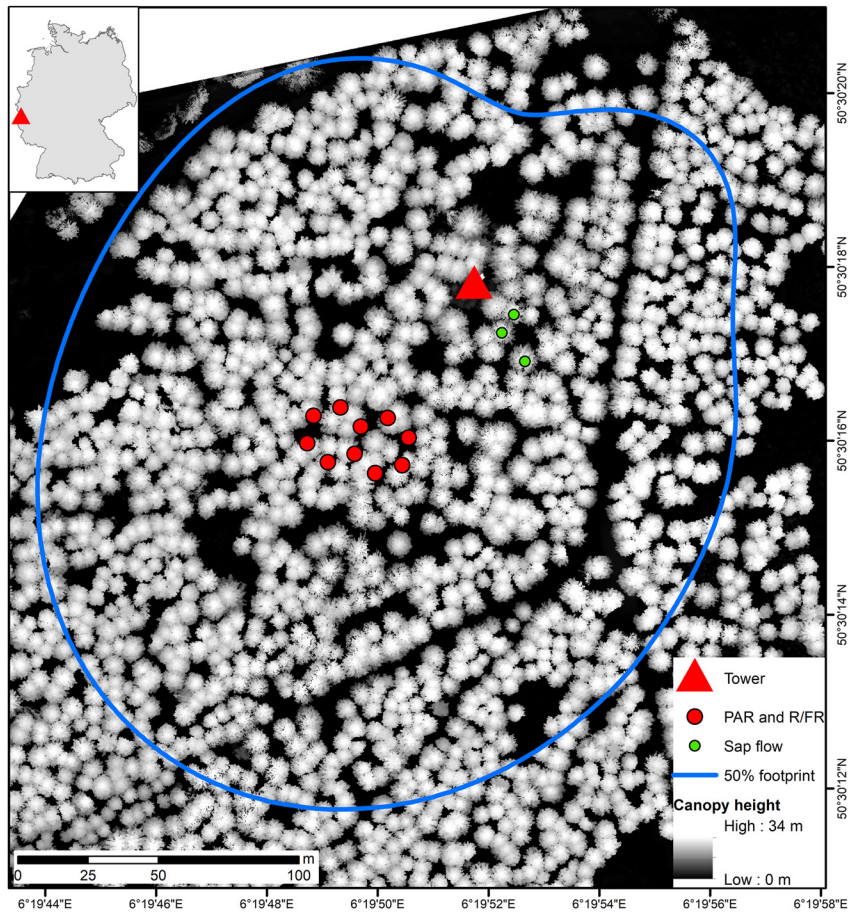

Figure 1. Light Detection And Ranging (LiDAR) derived canopy heights from the Wüstebach forest site, western Germany. LiDAR data collected on a March 2022 measurement campaign and were used for visualization only.

2.2. Eddy Covariance, Meteorological, and Sap Flow Measurements

Turbulent fluxes of CO_2, water vapor and sensible heat were measured with an eddy covariance system consisting of a sonic anemometer (CSAT-3, Campbell Scientific, Logan, Utah, USA) and an open-path infrared gas analyzer (LI-7500, LI-COR, Lincoln, Nebraska) with 15 cm sensor separation. The instruments were mounted at 38 m above ground on a tower above the forest canopy (Figure 1). Raw data recorded at 20 Hz were processed to 30-min fluxes with the software TK3 (Mauder & Foken, 2011), applying the strategy for quality control after Mauder et al. (2013), which includes tests for stationarity, well-developed turbulence, and source area representativeness. Following this, only data of the highest quality (flag 0) were retained and a storage flux estimated from single point CO_2 measurements was added. Post-processing was carried out using the *REddyProc* software package (Wutzler et al., 2018), which includes friction velocity filtering, gap filling and partitioning of net ecosystem exchange of CO_2 into ecosystem respiration (R_{eco}) and GPP. For partitioning, the method after Reichstein et al. (2005) was applied, which determines the temperature sensitivity of R_{eco} from nighttime data and extrapolates this to daytime.

Further environmental variables used for the analysis include measurements of global radiation (I) and diffuse radiation (d) measured at 34 m (NR01, Hukseflux Thermal Sensors, Delft, Netherlands), from which the diffuse fraction (d/I) was calculated. In addition, air temperature (T_{air}) and relative humidity (rH) were measured at 38 m (HMP45, Vaisala Inc., Helsinki, Finland), from which VPD was derived. From measurements of soil water content (SWC) in 2, 5, 10, 20, 50, and 80 cm depth (CS616, Campbell Scientific, Logan, Utah, USA) a root zone SWC weighted by thickness of layer was calculated as $SWC_{AVG} = (SWC_{02} * 3 + SWC_{05} * 4 + SWC_{10} * 7 + SWC_{20} * 20 + SWC_{50} * 30 + SWC_{80} * 36)/100$, where each subscript denotes the depth in cm to account for dynamic root growth (Y. Wang et al., 2021).

As an indicator of stomatal responses, sap flow density (J_S) was derived from three spruce trees about 20 m to the southeast of the tower (Figure 1). Each tree was instrumented with a Granier sensor comprising four needles (Ecomatik SF-L, Ecomatik, Dachau, Germany), mounted at 1.5 m height, from which the average J_S of the trees was derived from the temperature difference between two probes (Bogena et al., 2015; Neuwirth et al., 2021). The respective equation follows empirical relations (Granier, 1987):

$$J_S = 119 * \left(\frac{\Delta T_{max} - \Delta T}{\Delta T}\right)^{1.231}, \tag{1}$$

where J_S is the sap flow density (g m^{-2} s^{-1}), ΔT is the actual temperature gradient between the two probes and ΔT_{max} the maximum temperature gradient measured between the probes in a given time period. The length of this time period depends on the prevailing environmental conditions, because ΔT_{max} represents a state of zero sap flow. According to the manufacturer's recommendations (Ecomatik, 2005) we identified ΔT_{max} as the maximum ΔT of the vegetation period representing no radial tree-trunk increment and an rH of 100% with transpiration tending to zero. With these measurements, the relationships between J_S, VPD, and APAR were then analyzed to identify energy-limited and water-limited conditions for photosynthesis.

2.3. Sentinel-2 Derived Vegetation Indices

The normalized difference vegetation index (NDVI) was used for the estimation of APAR by green vegetation and CCC was used as an indicator of photosynthetic capacity to incorporate nutrient availability and past environmental conditions, especially the delayed response of chlorophyll content to suitable meteorological conditions in the early growing season (Gitelson et al., 2014). In order to estimate NDVI and CCC, Sentinel Level-2A bottom of atmosphere images between April and October 2021 were downloaded from Google Cloud via sen2r (Ranghetti et al., 2020). A mask was applied to filter out clouds and shadows, and the images were further visually inspected to exclude scenes with undetected clouds or cloud shadows over the study area, after which 13 scenes well distributed over the growing season remained. NDVI was calculated as

$$\mathrm{NDVI} = (B_{842} - B_{665}) / (B_{842} + B_{665}), \tag{2}$$

where the subscript denotes the wavelength in nm of the respective Sentinel-2 band (B), that is, band 8 (near infra-red) for B_{842} and band 4 (red) for B_{665}. For CCC, the 13 scenes were resampled to 20 m spatial resolution and processed with the Biophysical Processor in SNAP (https://step.esa.int/main/toolboxes/snap/) to yield LAI and C_{ab} products. The algorithm for biophysical variables included in SNAP consists of an artificial neural network trained with PROSAIL radiative transfer model input variables (Weiss et al., 2020). CCC was then derived by multiplying LAI with C_{ab} and for both NDVI and CCC pixel values of the woodlot were averaged. Finally, values from the 13 scenes were linearly interpolated to a daily scale.

2.4. PAR and R/FR Measurements

PAR was recorded instantaneously every 10 min with full-spectrum quantum sensors (SQ-521-SS, Apogee Instruments, Logan, Utah, USA) measuring the photon flux in the spectral range from 389 to 692 ± 5 nm. The sensors' error due to temperature response is below 2% for prevalent temperatures of the 2021 growing season (5°C–30°C). The R/FR ratio was recorded likewise with S2-431-SS sensors (Apogee Instruments, Logan, Utah, USA) measuring red light from 645 to 665 nm ± 5 and far-red light from 720 to 740 nm ± 5 nm. All PAR and R/FR sensors were connected to the wireless sensor network SoilNet (Bogena et al., 2010). Incident PAR (PAR_{in}) and outgoing PAR (PAR_{out}) and incident R/FR (R/FR_{in}) were measured with two opposite PAR sensors and one R/FR sensor above the forest canopy on a tower at 38 m above ground (Figure 1). In order to find a suitable field for measurements of transmitted PAR (PAR_{trans}) and R/FR (R/FR_{trans}) below the canopy, several criteria were set. According to these, the field had to be: (a) within the 50% cumulative source area of the eddy covariance station as calculated after Kormann and Meixner (2001), (b) at least 80 m away from the forest edge to minimize the influence of lateral radiation fluxes, and (c) representative of the general woodlot comprising the 50% footprint area in terms of canopy density. For the latter, a Light Detection And Ranging (LiDAR) point cloud from Geobasis NRW was used and the ratio of above ground to total LiDAR points for each 30-m cell of the woodlot was calculated. A representative cell was identified as being within one standard deviation from the mean ratio of the whole woodlot. Based on these criteria, a measurement field 70 m to the southwest of the tower was chosen

(Figure 1). There, 10 PAR sensors were mounted on tripods in 1.3 m height and arranged with 10 m distance in two hexagons to maximize the sensing area (Putzenlechner, Marzahn, et al., 2019) and one of these hexagons was also equipped with six R/FR sensors.

For calculating APAR, cases with $PAR_{trans} > PAR_{in}$ were excluded as a sign of cloud cover only above the tower. High wind speeds can induce an increase of the sampling error of PAR_{trans} measurements from a limited number of sensors during direct light conditions (Putzenlechner, Marzahn, et al., 2019). This sampling error is caused by the high spatial variability of forest canopies (Leuchner et al., 2011; Widlowski, 2010). Therefore, the fAPAR was calculated first and filtered for low wind speeds (<5 m s^{-1}), and data gaps were linearly interpolated. We also considered reducing the sampling error further by filtering for diffuse light conditions (d/I > 0.9). However, important conditions such as the highest VPD typically occur during direct light conditions, and only considering diffuse light would also ignore the bowl-shaped diurnal cycle of fAPAR during direct light (Widlowski, 2010). The domain-level fAPAR was calculated as a two-flux product instead of a three-flux product because in this way the bias to fAPAR from all four flux terms is expected to be smaller (Putzenlechner et al., 2020; Widlowski, 2010):

$$\mathrm{fAPAR} = \frac{1}{n}\sum_{i}^{n} 1 - \mathrm{PAR}_{\mathrm{trans}_i}/\mathrm{PAR}_{\mathrm{in}}, \tag{3}$$

where i is the sensor location of each PAR_{trans} sensor, however, without measurements from one sensor due to malfunctioning ($n = 9$). APAR of green parts of the tree canopy was then calculated as

$$\mathrm{APAR}_g = \mathrm{PAR}_{\mathrm{in}} * \mathrm{fAPAR} * \mathrm{NDVI}, \tag{4}$$

for which each 10-min values of PAR_{in} and fAPAR were linked to the NDVI values of the corresponding day. NDVI was used for the proportion of green vegetation because of its normalized nature and utility in previous research to estimate $APAR_g$ (Nestola et al., 2016).

Data from the six R/FR sensors were averaged for the calculation of R/FR_{trans}. As R/FR is strongly dependent on solar elevation and the precipitable water vapor in the atmosphere, which attenuates light in the far-red but not in the red domain (Doroszewski et al., 2015; Kotilainen et al., 2020), we also calculated the difference between the R/FR ratios above and below the canopy as $R/\mathrm{FR}_{\mathrm{diff}} = R_{\mathrm{in}}/\mathrm{FR}_{\mathrm{in}} - R_{\mathrm{trans}}/\mathrm{FR}_{\mathrm{trans}}$ to represent the change of the spectral ratio caused by the canopy alone. All radiation data were filtered for daytime conditions ($PAR_{in} > 10$ μmol m^{-2} s^{-1}) and linked to GPP estimates by aggregating them to 30-min values. Finally, green LUE was calculated as

$$\mathrm{LUE}_g = \mathrm{GPP}/\,\mathrm{APAR}_g. \tag{5}$$

2.5. Evaluation of Environmental Drivers

LUE_g was calculated at the half-hourly scale and at the daily scale from daytime integrals of GPP and $APAR_g$. Half-hourly LUE_g, however, has the problem of being skewed because a ratio is more affected by changes of the denominator ($APAR_g$), especially if it is low (Hedges et al., 1999). At the daily scale, the range of $APAR_g$ was much smaller, and hence the dependence on $APAR_g$ was not as dominant (see Figure S1 in Supporting Information S1). For this reason it is necessary to present half-hourly LUE_g with a log10-transformed y-axis so that LUE_g is affected equally by changes of the numerator and denominator. However, Feng et al. (2014) stated to use log-transformations with caution as statistical modeling on those data may not be relevant for the original data. Therefore, we also provide an alternative approach in Supporting Information S1, that uses deviations of GPP from a year- and site-specific optimal GPP (GPP_{opt}) in relation to $APAR_g$ instead (see Text S1 and Figures S2 and S3 in Supporting Information S1).

In order to robustly quantify the importance of environmental variables for predicting half-hourly daytime GPP, two different feature importance measures based on different machine-learning algorithms were applied. First, permutation importance based on random forest (RF, Breiman, 2001), and second, SHapley Additive exPlanations (SHAP) values (Lundberg & Lee, 2017) based on gradient boosting (GB, Friedman, 2002). Both RF and GB have the advantage of capturing even highly non-linear relations between target and predictors and are based on an ensemble of decision trees. For RF, all trees are grown independently with a random subsample of data, while the trees for GB are built based on the errors of the previous tree in order to minimize a loss function. The

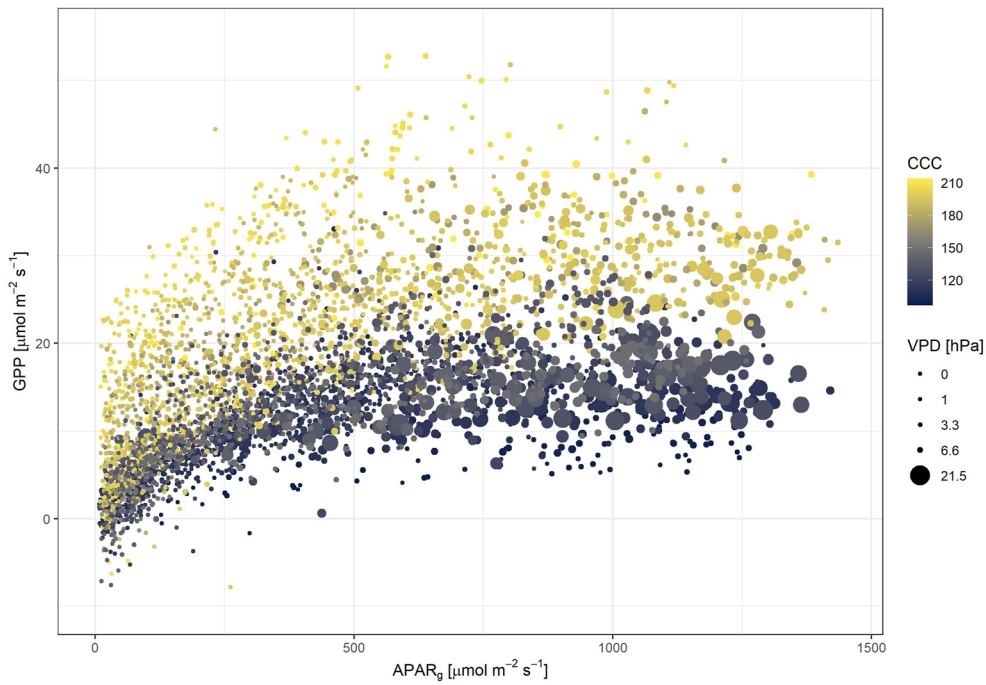

Figure 2. Gross primary productivity (GPP) against green canopy absorbed photosynthetically active radiation ($APAR_g$) during the 2021 growing season, colored by canopy chlorophyll content (CCC) and dot sizes by Vapor pressure deficit (VPD).

permutation importance is assessed by randomly shuffling the values of each variable and measuring the decrease in prediction accuracy. To avoid a bias from correlated predictors, we used the conditional permutation scheme of Strobl et al. (2008), where values are permuted within a grid of correlated variables. For this, we applied the latest version of this algorithm in the *permimp* package in *R*, which also considers non-linear dependence between variables (Debeer & Strobl, 2020), based on the conditional inference trees implementation of RF in *cforest* (Hothorn et al., 2006). SHAP is a local method to explain the importance for individual predictions by unifying various Shapley value methods, which use equations from game theory to fairly allocate rewards. For this study, we applied SHAP via *SHAPforxgboost* (Liu & Just, 2021) based on the *XGBoost* implementation of GB (Chen & Guestrin, 2016). For both models, only non-gap-filled values were considered and hyperparameter tuning and a random 5-fold cross-validation was conducted with *caret* (Kuhn, 2008). As RF and GB are subject to random variation, the procedures were repeated 10 times and results were averaged to produce more robust estimations.

3. Results

3.1. Interpretation of Environmental Drivers

The efficiency by which $APAR_g$ is used for photosynthesis is observed by a light response curve of GPP (Figure 2). For each $APAR_g$ domain, a wide range of GPP values was recorded. Low GPP values at a particular $APAR_g$ corresponded well with a low CCC, indicating a limiting effect on photosynthetic capacity. In general, GPP displays an increasing trend with increasing $APAR_g$ until about 600 μmol m^{-2} s^{-1}, after which a saturation of APAR occurred. The larger circles further show that many of the lowest GPP values at high APAR coincided with high VPD, most of them during a warm and dry spell in June.

The good agreement between CCC and GPP can also be seen in time series (Figures 3b and 3c) and a scatterplot (Figure S4a in Supporting Information S1). In Figure 3, no significant increase of GPP, LUE_g or CCC can be noticed until mid-June. In mid-July and mid-August, however, LUE_g exhibited two marked peaks with a minimum in between. $APAR_g$ and J_S had a high day-to-day variation while T_{air} and VPD peaked in mid June. Over the whole research period, daily LUE_g was 4.0% ± 2.3%, with daily values ranging from 0.7% to 12.1%. Out of total APAR, the LUE was 3.1% on average, and of PAR_{in} just 2.8%.

In general, the response to environmental drivers was similar for half-hourly and daily LUE_g. T_{air} had a relatively clear optimum around 15°C for both 30 min and daytime averages, though even around 15°C low LUE_g values

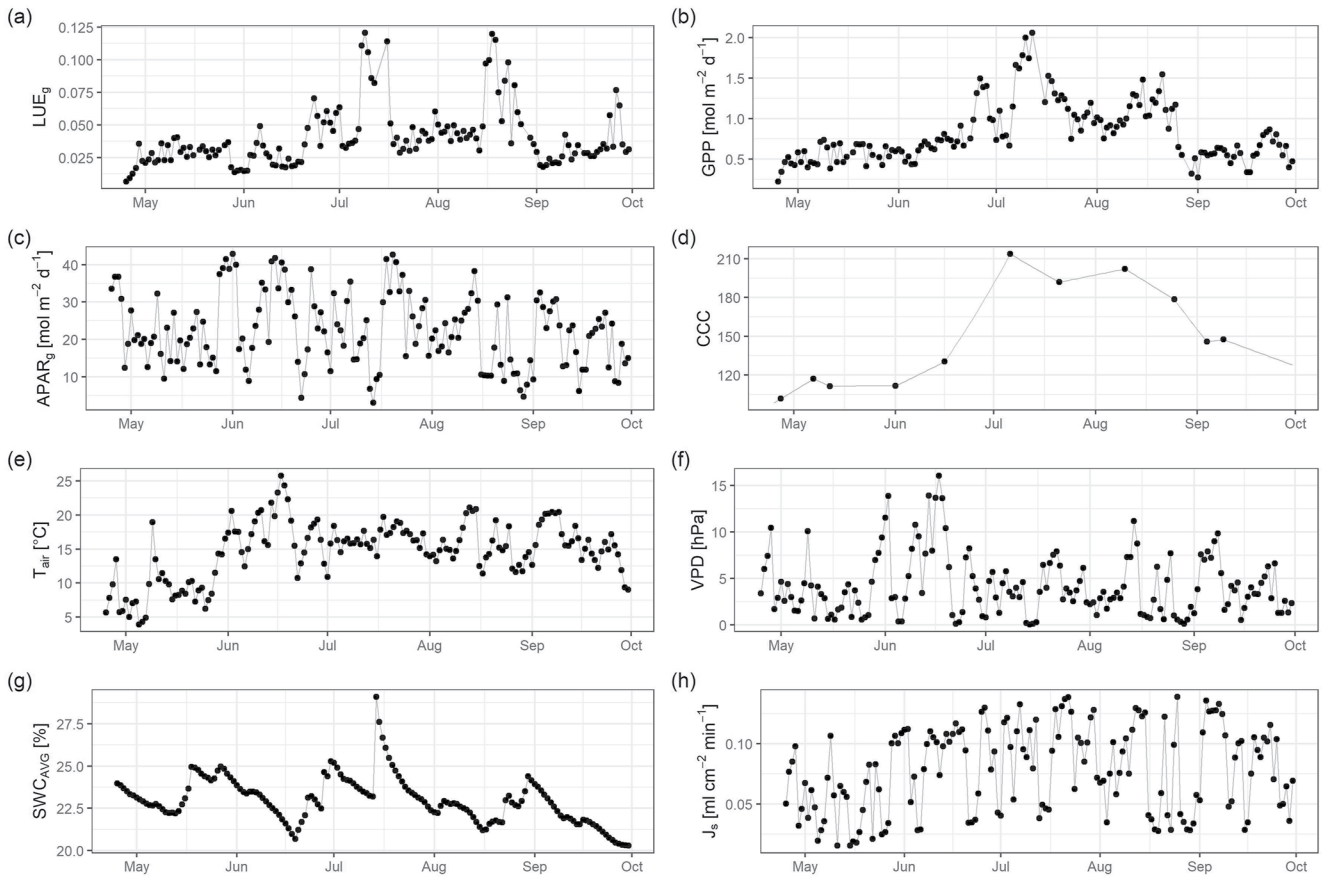

Figure 3. Time series of daily averaged daytime values of (a) green canopy light use efficiency (LUE_g), (b) gross primary productivity (GPP), (c) green canopy absorbed photosynthetically active radiation ($APAR_g$), (d) canopy chlorophyll content, (e) air temperate (T_{air}), (f) Vapor pressure deficit, (g) soil water content (SWC_{AVG}), and (h) sap flow density (J_S) from 20 April to 30 September. For LUE_g and GPP, only those days with at least 25% non-gap-filled GPP data were considered.

were observed (Figures 4a and 4b). Half-hourly LUE_g was rather insensitive to VPD until it reached values above about 7.5 hPa, after which a decrease was noticeable. For daily LUE_g a similar pattern was evident, although the decrease started at daytime averaged VPD > 3 hPa (Figures 4c and 4d). Half-hourly and especially daily LUE_g were higher during diffuse compared to direct light conditions. Similarly, they tended to be higher when R/FR_{diff} was lower (Figures 4e–4h), meaning that the ratio was shifted comparatively less to the far-red spectrum after passing the canopy. However, neither showed a clear response to SWC_{AVG} (Figures 4i and 4j).

3.2. Importance of Environmental Drivers for Machine Learning Models

The results from permutation importance and SHAP agree well, indicating that the importance estimations can be considered robust. For both approaches, CCC was the most valuable feature for predicting GPP closely followed by $APAR_g$ (see Figure 5). Though only according to SHAP, SWC_{AVG} had a higher importance than the remainder variables. RF and GB both could reproduce GPP well within a 5-fold random cross-validation, resulting in an R^2 of 0.83 for RF and 0.84 for GB (Figure S5 in Supporting Information S1), though this does not tell how good the models are for spatiotemporal extrapolation. However, when replacing $APAR_g$ and CCC by the rough proxies of SZA and day of year (DOY), the RF model performance drops only to an R^2 of 0.81 with SZA and DOY as the most important variables (see Figure S6 in Supporting Information S1). A RF model with neither of them, on the other hand, has only an R^2 of 0.56. This leads to the impression that the diurnal and seasonal information contained in $APAR_g$ and CCC are more important than their specific quantities.

The analysis of individual SHAP values further revealed that high CCC values yielded higher GPP predictions and the limiting effect of low APAR was also evident. Dependence plots of SHAP values of each variable give a more detailed view, especially for variables with a rather small range of SHAP values (see Figure S7 in Supporting

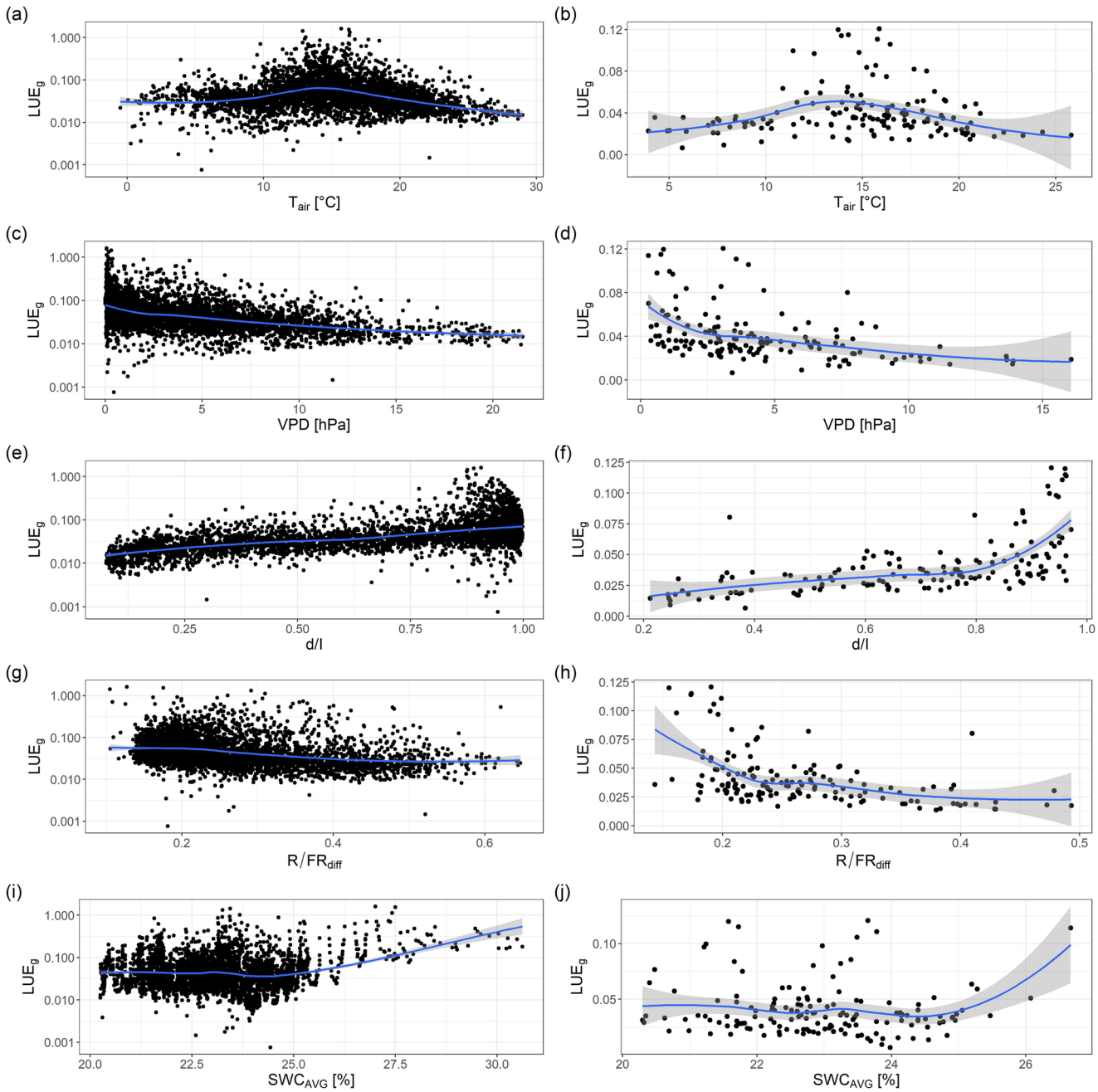

Figure 4. Green canopy light use efficiency (LUE_g) at a half-hourly scale with log10-transformed *y*-axes (left) and at a daytime scale (right) against (a and b) air temperature, (c and d) vapor pressure deficit, (e and f) diffuse fraction, (g and h) red to far-red ratio difference between above and below canopy, and (i and j) soil water content, each with a locally estimated scatterplot smoothing function in blue and a 0.95 confidence interval in gray. For daily LUE_g, only those days with at least 25% non-gap-filled gross primary productivity data were considered.

Information S1). Here, it is notable that both very low and high VPD yielded a low GPP outcome, while high and low SWC_{AVG} values are related to high GPP outcomes.

3.3. Sap Flow—GPP Relationship and Their Response to Environmental Drivers

The correlation of J_S to GPP in relation of VPD and CCC is shown in Figure 6. Half-hourly periods with high GPP despite very low J_S (<0.025 ml cm^{-2} min^{-1}) occurred on very low maximum daily VPD (VPD_{mx}) days (Figure 6a), indicating that J_S and GPP were not correlated when photosynthesis required little transpiration. For

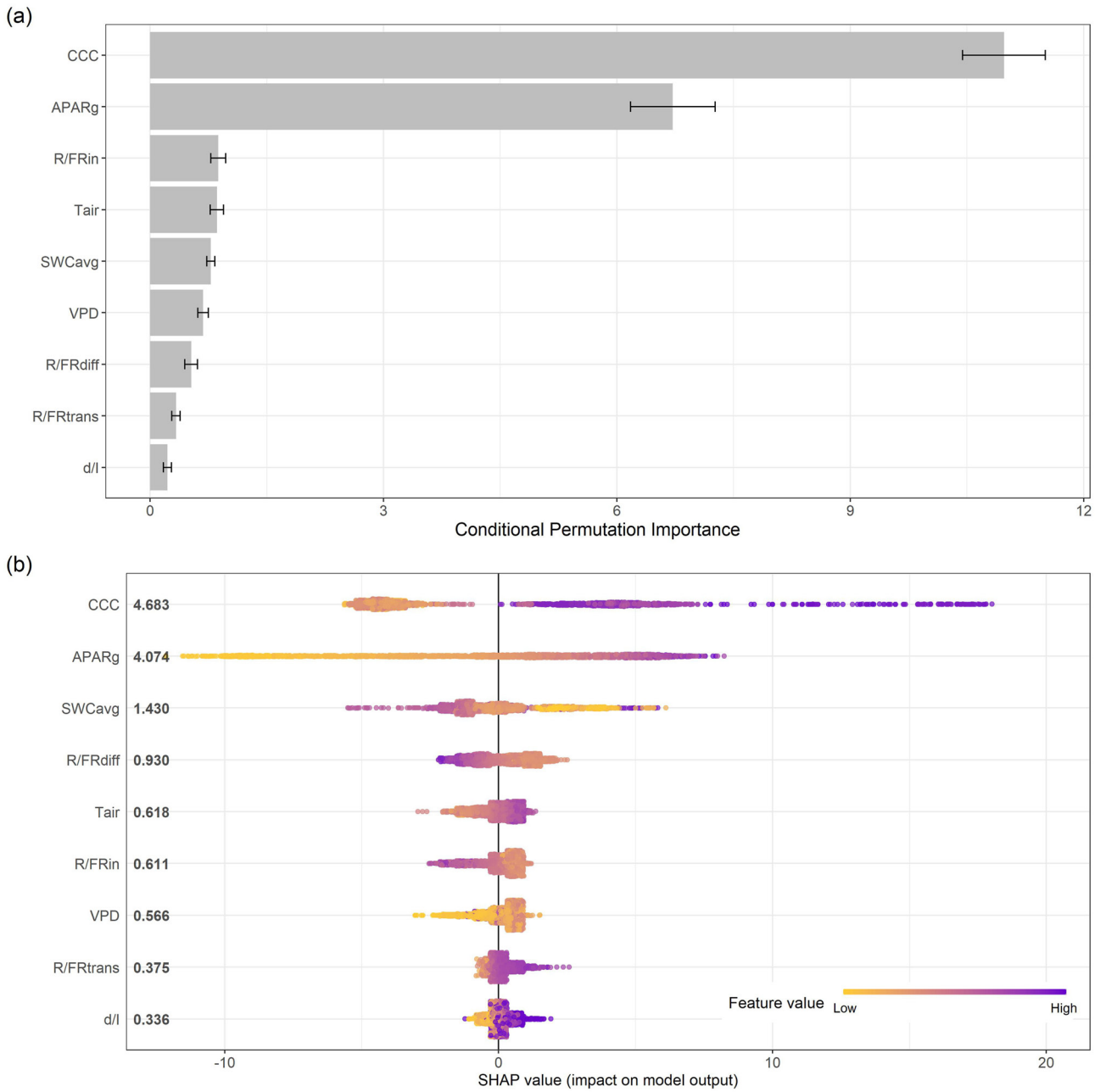

Figure 5. Average conditional permutation importance (unitless) of environmental variables for a random forest gross primary productivity (GPP) model with error bars displaying one standard deviation between 10 iterations (a), and SHapley Additive exPlanations (SHAP) values of those variables for a gradient boosting GPP-model (b). The more values deviate from 0, the more important was the respective variable for the prediction, with negative values related to low GPP outcomes. Numbers on the left show the average absolute SHAP value (unitless) of each variable. R^2 of a random 5-fold cross-validation of the models was 0.83 for random forest and 0.84 for gradient boosting.

a given value of J_S above 0.05 ml cm^{-2} min^{-1}, GPP was generally lower on high VPD$_{mx}$ days and likewise for the same GPP, a higher J_S occurred on high VPD$_{mx}$ days. In the relation to VPD, J_S showed a strong increase with increasing VPD until about 7.5 hPa were reached, after which J_S seems to be capped and even showed a slightly decreasing trend for VPD > 12.5 hPa (Figure 6b). However, even at low VPDs, J_S was within a broad range of about 0.1 ml cm^{-2} min^{-1}. Lower J_S values corresponded well to low CCC, indicating a limiting influence on sap flow potential. Extraordinarily low J_S values stand out at moderate VPD values of about 10 hPa. These values correspond to low sun angles (SZA > 70°; star symbol in Figure 6b) and occurred in the early morning after nights during which VPD remained relatively high but APAR and thus J_S were still low.

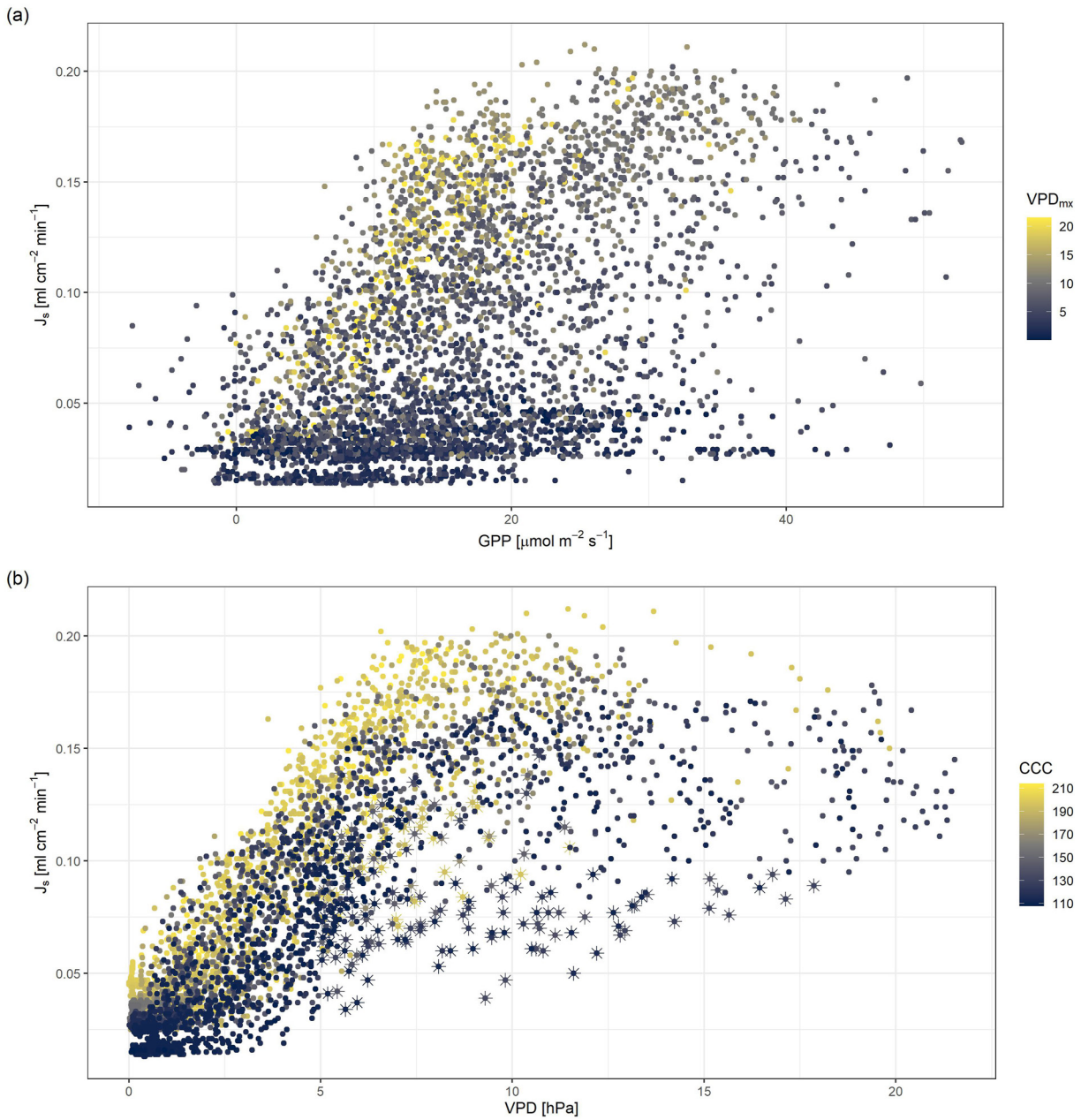

Figure 6. Sap flow density (J_S) against gross primary productivity colored by daily maximum vapor pressure deficit (VPD_{mx}) (a) and J_S against VPD colored by canopy chlorophyll content (b). The star symbols in panel (b) represent observations with solar zenith angle > 70° and VPD > 5 hPa.

The hysteretic responses of J_S and GPP to VPD and $APAR_g$ are shown in Figure 7 for different VPD_{mx} classes. The averaged hysteresis of J_S to VPD showed markedly different patterns for different VPD_{mx} domains. For VPD_{mx} < 1.5 hPa (not shown), a chaotic pattern generally dominated, though for days with VPD_{mx} between 1.5 and 5 hPa, an anti-clockwise pattern with higher J_S later in the day at same VPD could be observed (Figure 7a). A transitional pattern occurred for days with VPD_{mx} between 5 and 9 hPa without a clear hysteresis or just a clockwise loop around midday (Figure 7b). On VPD_{mx} days between 9 and 15 hPa, instead, a clear clockwise pattern with lower J_S later in the day at the same VPD levels was visible (Figure 7c). For days with VPD_{mx} above 15 hPa, the clockwise hysteresis was even more pronounced, and a decreasing J_S despite further rising VPD in the early afternoon occurred (Figure 7d). GPP, on the other hand, always showed a clockwise response to VPD independent of the VPD_{mx} scale (Figures 7e–7h). In the response to $APAR_g$, however, J_S and GPP both showed a clockwise pattern on high VPD_{mx} days. Though on lower VPD_{mx} days, GPP did not have a time lag toward

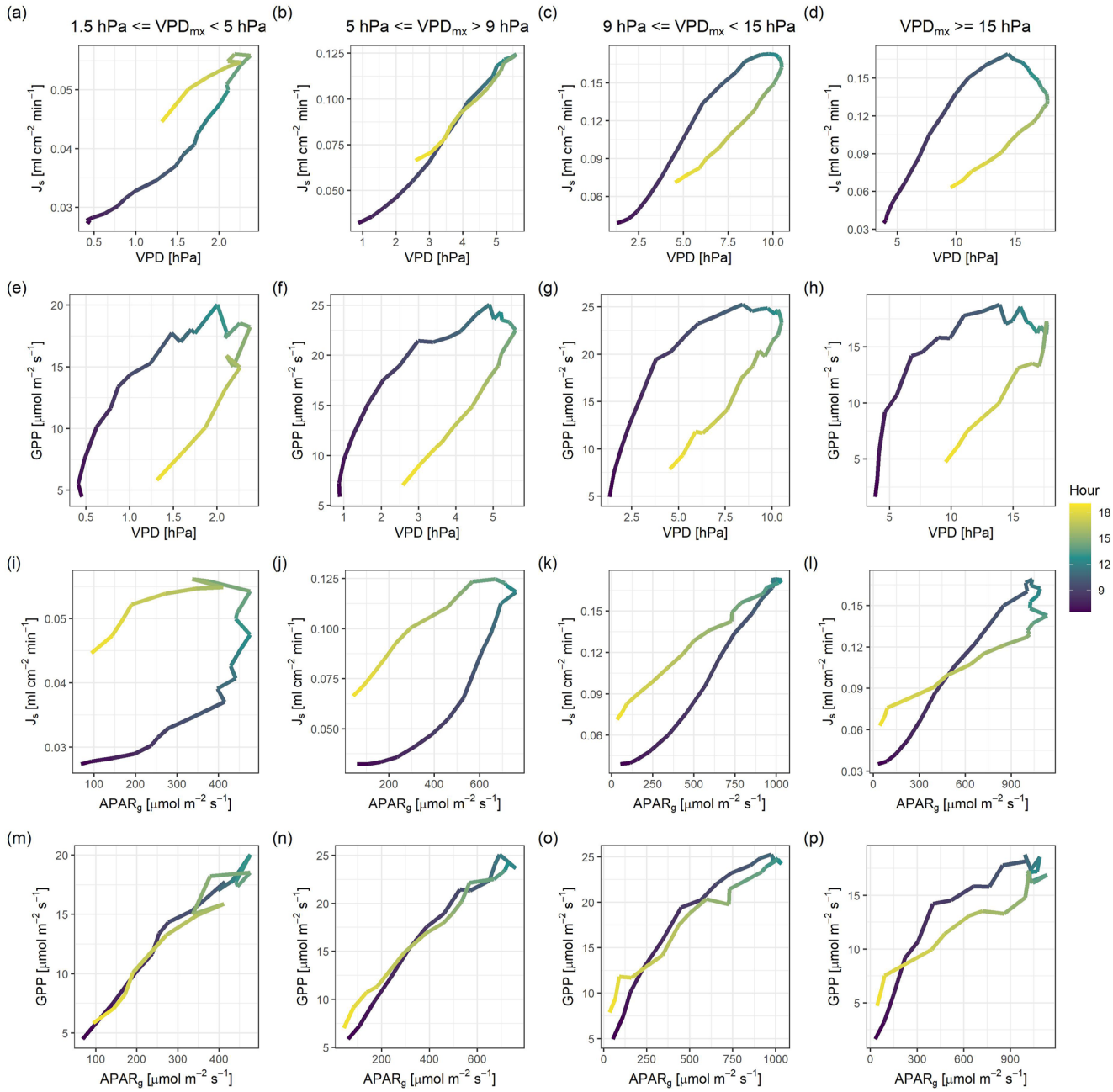

Figure 7. Hysteresis plots between (a–d) sap flow density (J_S) and vapor pressure deficit (VPD), (e–h) gross primary productivity (GPP) and VPD, (i–l) J_S and green canopy absorbed photosynthetically active radiation ($APAR_g$), and (m–p) GPP and $APAR_g$, averaged for four different daily maximum VPD classes (columns). A clockwise (anti-clockwise) pattern occurs if afternoon and evening values of J_S or GPP are higher (lower) than in the morning at the same VPD or $APAR_g$.

$APAR_g$, while J_S had an anti-clockwise pattern that shifted toward a clockwise pattern with increasing VPD_{mx} (Figures 7i–7p).

4. Discussion

4.1. Identification of Photosynthesis Limiting Conditions

Besides this study, an anti-clockwise hysteretic response of J_S to VPD was reported only for *P. sylvestris* growing in a wet and cool climate (H. Wang et al., 2019). This hysteretic response has not been found for plants in tropical

(Motzer et al., 2005; Roddy, 2013) or semi-arid climates (Li et al., 2016; Zha et al., 2017). A delayed response of J_S to VPD can be explained by the use of water stored in the upper stem during the morning hours (Goldstein et al., 1998; Perämäki et al., 2005). Stored water is only sufficient on low VPD and $APAR_g$ days, and is not detected by sap flow measurements usually carried out at 1–1.5 m height (H. Wang et al., 2019). We hence interpret the shift of the J_S response to VPD from anti-clockwise to clockwise as a sign of non-sufficient water storage in the upper plant. Main possible reasons for afternoon stomatal closure causing a clockwise response of J_S to VPD given by previous studies (O'Brien et al., 2004; Zeppel et al., 2004; Zhang et al., 2014) can be summarized to: (a) a declined soil–root conductance due to decreased SWC, (b) a higher stomatal sensitivity to VPD due to changed water potential gradients or xylem sap chemical composition, and (c) decreased $APAR_g$, caused by the delay of VPD to radiation resulting in higher $APAR_g$ values earlier in the day at a given VPD (see Figure S8 in Supporting Information S1).

Given that GPP showed a clockwise response to VPD even on very low VPD_{mx} days, we conclude that a decrease of $APAR_g$ and hence stomatal closure induced by energy limitations is the main cause for such cases at this particular site. This means that for higher VPD_{mx} days a clockwise J_S-VPD pattern by itself is not a sufficient indicator for water stress or atmospheric demand induced stomatal closure. The decrease of J_S despite increasing VPD only on the highest VPD_{mx} days can be considered a clearer sign of such conditions. As photosynthesis is primarily driven by $APAR_g$, the non-hysteretic response of GPP to $APAR_g$ on low VPD_{mx} days seems reasonable. Since J_S is likewise driven by $APAR_g$, but also scaled by VPD, which is typically highest in the afternoon, a slight anti-clockwise response to $APAR_g$ can be expected (Zeppel et al., 2004) that is also enhanced by the use of stem water in the morning. Hence, the shift to a clockwise pattern of both GPP and J_S to $APAR_g$ only on the highest VPD_{mx} days can be regarded as a good indicator of stomatal closure related to high atmospheric water demand at this site and year. Water-limited conditions, however, also depend on soil water potential, which can only be roughly estimated for this site. According to the soil water retention curve for the dominant silt loam texture after Tuller and Or (2004), even the minimum SWC_{AVG} of 20.3% during the 2021 growing season would have resulted in a pressure head of no less than about −10 m.

Limiting conditions for photosynthesis can also be identified by a time series of the relevant variables (see Figure 3 and Figure S9 in Supporting Information S1). For example, 12 June saw a marked minimum of $APAR_g$ around noon, which was likewise evident for VPD, J_S and GPP, demonstrating an energy-limited response. During a high $APAR_g$ period from 14 to 19 June with the highest VPD values (21.5 hPa) recorded during the whole growing season, both J_S and GPP were lower than during 25–28 June with distinctively lower VPD (<12.5 hPa). This could be interpreted as a water-limited response. However, the photosynthetic capacity also increased markedly from mid to late June (Figure 3d), complicating the analysis. For the hysteretic response differing CCC is not an issue as GPP and J_S are compared within the same day. In summary, the analysis of the J_S response especially to $APAR_g$ can reveal useful information to identify photosynthesis limiting conditions, although GPP and J_S are not always related as shown by discrepancies during very low VPD conditions.

4.2. Environmental Drivers

Both machine learning analyses show the consistency of CCC as the most important environmental variable for GPP. This high ranking also reveals that even for evergreen trees, meteorological drivers alone may not be sufficient to explain the variability in GPP. Moreover, a variable containing seasonal information about photosynthetic capacity will be also required. Our results are in agreement with previous research for mixed forests and maize crops (Croft et al., 2015; Gitelson et al., 2014; Peng et al., 2011). The higher importance of CCC even over $APAR_g$ agrees with the results from Wu et al. (2022). However, other variables influencing photosynthetic capacity, such as atmospheric CO_2 concentrations, were not included in the analysis (Dusenge et al., 2019; Farquhar et al., 1980). Furthermore, Cabon et al. (2022) showed that wood growth in contrast to GPP is more limited by water stress than temperature-related leaf phenology.

As for environmental drivers of LUE_g, we found a unimodal response to T_{air} with decreasing LUE_g at high temperatures. With this analysis, however, it is not possible to single out the effect of a specific variable on LUE_g because co-dependencies between variables occur. High values of T_{air} were strongly correlated to high VPD values (89% of T_{air} > 25°C had VPD > 15 hPa). Nevertheless, the observed decrease of LUE_g can also be caused by high T_{air} alone due to higher photorespiration in relation to photosynthesis with increasing leaf temperatures (Long, 1991), a process which also relates to high $APAR_g$. Likewise, as summarized by Bao et al. (2022), the temperature

sensitivity has been represented by bell-shaped functions many times in LUE-models though with differing optimum ranges (e.g., Horn & Schulz, 2011; Stocker et al., 2020; Xiao et al., 2004). Otherwise, it was also modeled by a linearly increasing function that reaches a plateau at ca. 16°C (Mäkelä et al., 2008).

VPD was overall not a very important variable for machine learning models despite its impact on stomatal conductance as shown by the sap flow analysis. This discrepancy can be attributed to the fact that the site is typically energy-rather than water-limited (Graf et al., 2014) with a particular cool and wet 2021 growing season. This resulted in many low VPD observations that were rather indifferent to LUE_g, though nonetheless some high VPD days occurred that restricted stomatal conductance. The wet growing season probably also explains the relatively low importance of SWC, which reacts slower to dry periods with increasing depth (Xu et al., 2021). In comparison, for a drought-affected tropical dry forest, a high importance of VPD and latent heat flux to explain GPP was detected by Castro et al. (2018). A similar response to VPD as ours, that is, a decrease of LUE only at VPD above ca. 5 hPa, was found by Horn and Schulz (2011), while others found an immediate decrease of LUE with increasing VPD (Kalliokoski et al., 2018; S. Wang et al., 2018). Likewise, Fu et al. (2021) showed that during soil moisture dry downs, the covariance between GPP and VPD was positive at first, and changed to negative only after a certain soil moisture threshold was surpassed. The low LUE_g values even within the optimum range of environmental variables such as T_{air} shows those are necessary but not sufficient conditions. During the occurrence of highest GPP and LUE_g values in mid-July and mid-August all or most environmental drivers likely were within their optimal range.

While half-hourly LUE_g showed only a modest increase with d/I, which is also reflected in a low importance for machine learning models, daily LUE_g was significantly higher during diffuse light conditions (Figure 4f). A similar response was observed to low R/FR_{diff} and both were highly correlated (correlation coefficient of −0.92; see also Figure S4b in Supporting Information S1). This is probably linked to lower $APAR_g$ values during diffuse light and therefore less excessive light. Besides that, an enhancement of LUE_g under diffuse conditions has been linked to a smaller fraction of the canopy in deep shade (Williams et al., 2014) and previous research showed that coniferous forests can also be larger CO_2 sinks under diffuse conditions (Law et al., 2002; Urban et al., 2007, 2012). A linear increase between cloudiness and LUE was hence included in LUE-models (S. Wang et al., 2018), though Bao et al. (2022) found an exponential increase more suitable that also fits better with our results. As the R/FR ratio was always shifted to FR after passing the canopy but less so during diffuse conditions, obscured parts of the canopy received not only a higher light quantity, but also a higher light quality than under clear skies. Such a vertical R/FR profile was shown for spruce trees by previous research (Dengel et al., 2015; Hertel et al., 2011), and in this way the higher LUE_g at small R/FR_{diff} might not be attributed to higher d/I and less excessive light alone.

4.3. Variability and Uncertainties of LUE_g Estimates

Variation of LUE_g shown in Figure 3a can primarily be attributed to variations of $APAR_g$ and GPP. $APAR_g$ was predominantly dependent on fluctuating cloud cover patterns, while GPP likely was influenced by various current and past environmental drivers (see Section 3.2). LUE_g remained within a rather low range between late April and late June. This can be attributed to below average temperatures in April and May with a subsequent low CCC well into June, as well as a warm and dry period with comparatively high VPD values in mid-June probably causing water-related stomatal closure (see Section 3.3). As the first peak of GPP corresponds to an increase of CCC as well as low VPD, we attribute this peak to the probably first suitable growing conditions after cold temperatures in May and dryness in June. The first LUE_g drop in late July saw decreasing $APAR_g$, GPP, T_{air}, and CCC (although from few observations) and thus may be related to energy-limited conditions. The second GPP and LUE_g peak did not occur during the same days. A peak of GPP occurred from 12 to 15 August but was associated with relatively high $APAR_g$ values and thus did not result in a high LUE_g. The LUE_g peak instead occurred from 16 to 19 August with only moderate GPP (1.03–1.24 mol m^{-2} d^{-1}) during the rapid onset of very low and consistent $APAR_g$ in consequence of the passage of the low pressure system *Luciano*. Explaining why GPP did not likewise decrease to lower values is beyond this analysis. However, the low amounts of PAR_{in} were perhaps still enough to sustain a moderate GPP. The last drop of GPP in late August then is accompanied by a continuous decrease of CCC, which can be interpreted as the onset to the end of the growing season.

GPP derived from eddy covariance measurements is subject to well-known limitations including the difficulty of estimating a storage term without a vertical CO_2 profile (Montagnani et al., 2018), the identification of vertically

decoupled flows (Peltola et al., 2021), and the uncertainty from partitioning net ecosystem exchange into GPP and R_{eco} (Raj et al., 2016). PAR_{trans} measurements from a limited number of sensors were subject to a sampling error during direct light conditions, as indicated by a non-flattening curve of the coefficient of variation as a function of the number of sensors (see Figure S10 in Supporting Information S1). Additionally, a bias to an ideal APAR calculated from all PAR flux terms can be expected (Widlowski, 2010). In our case, we did not measure horizontal and ground-reflected PAR fluxes. Green APAR has the advantage over total APAR that only light actually useable for photosynthesis is considered. In this way, the effect of short-term drivers such as VPD and T_{air} on the partitioning of energy in photosynthesis and, for example, transpiration, non-photochemical quenching, and fluorescence can be investigated. However, environmental conditions causing a reduction of NDVI such as drought, insect infestation or wind storms will not properly be reflected in a decreased LUE_g. With total APAR, these conditions would decrease LUE as long as the canopy surface area is not reduced. Chlorophyll content, on the other hand, can be low despite an apparently "green" leaf (Gitelson & Gamon, 2015). Hence it is important for GPP models that PAR absorbable by chlorophyll might still be overestimated by NDVI-based $APAR_g$ and thus LUE_g underestimated. The Sentinel-2 derived NDVI estimates induce a further uncertainty to $APAR_g$, although a validation with in situ measurements showed the reliability of Sentinel-2 NDVI (Lange et al., 2017). By measuring PAR_{trans} in 1.3 m, the light used for photosynthesis by the ground vegetation was not included in fAPAR, though their productivity was included in GPP. The contribution of ground vegetation to GPP, however, can be expected minor in an old growth forest stand (Kulmala et al., 2011). Excluding photosynthesis of ground vegetation would hence slightly decrease LUE_g, which is a counterweight to the former limitation. Although calculating LUE as in Equation 5 is most straightforward and commonly used (e.g., Gitelson & Gamon, 2015; Martini et al., 2022; Wieneke et al., 2018), LUE can also be assessed by metrics of the light response curve, such as the initial slope or the half saturation point (Williams et al., 2014). In addition, the SQ-521-SS sensors measured PAR from 389 to 692 nm, though Zhen and Bugbee (2020) argued to include FR light (701–750 nm) in the definition of PAR, as FR causes a balanced excitation of the two photosystems, and hence improves photochemical efficiency.

5. Conclusions

Our study found that (a) a seasonal variable such as CCC is consistently necessary for accurate GPP estimations by machine learning models and hence should be considered as a possible improvement for LUE-based approaches and (b) tree-scale J_S and ecosystem-scale GPP showed a congruent clockwise hysteretic response to $APAR_g$ on high VPD days, thus likely being a good indicator of water stress induced stomatal closure. In this way, this novel dual-scale comparison of hysteretic cycles has the potential to be of general value for identifying photosynthesis-limiting conditions. We anticipate these findings will be valuable for the development of GPP-modeling approaches, and can serve as a basis to be confirmed by multi-site and multi-year studies across different environments and climate zones.

Acknowledgments
The project was co-funded under the Excellence Strategy of the Federal Government and the Länder (Project ComRadE, SFUoA002) and the University of Alberta, Canada / RWTH Aachen University, Germany. The research was also funded by the Waldklimafonds (project MW3; Grant agreements 2220WK86A4 and 2220WK86B4). The Waldklimafonds itself is funded by the German Federal Ministry of Food and Agriculture (BMEL) and Federal Ministry for the Environment, Nature Conservation, Nuclear Safety and Consumer Protection (BMUV) administrated by the Agency for Renewable Resources (FNR). The basic equipment of the Wüstebach site with measurements was funded by the TERENO project (www.tereno.net). We acknowledge support from the Helmholtz research infrastructure Modular Observation Solutions for Earth Systems (MOSES). In particular, we thank Marius Schmidt, Ansgar Weuthen, Bernd Schilling, Daniel Dolfus, and Martina Kettler for installation and maintenance of the radiation sensors and the eddy covariance system, Carsten Montzka for gathering and processing LiDAR data, and Lutz Weihermüller for providing soil properties. We thank two anonymous reviewers who helped to improve the manuscript substantially. Open Access funding enabled and organized by Projekt DEAL.

Data Availability Statement

Associated data are available at http://doi.org/10.5281/zenodo.7014604. LiDAR data used in this study can be freely accessed at https://www.opengeodata.nrw.de/produkte/geobasis/hm/3dm_l_las/3dm_l_las/ and Sentinel-2 data can be freely accessed at https://scihub.copernicus.eu/.

References

Ammer, C. (2003). Growth and biomass partitioning of Fagus sylvatica L. and Quercus robur L. seedlings in response to shading and small changes in the R/FR-ratio of radiation. *Annals of Forest Science*, *60*(2), 163–171. https://doi.org/10.1051/forest:2003009

Anav, A., Friedlingstein, P., Beer, C., Ciais, P., Harper, A., Jones, C., et al. (2015). Spatiotemporal patterns of terrestrial gross primary production, A review. *Reviews of Geophysics*, *53*(3), 785–818. https://doi.org/10.1002/2015RG000483

Archer, K. J., & Kimes, R. V. (2008). Empirical characterization of random forest variable importance measures. *Computational Statistics & Data Analysis*, *52*(4), 2249–2260. https://doi.org/10.1016/j.csda.2007.08.015

Bao, S., Wutzler, T., Koirala, S., Cuntz, M., Ibrom, A., Besnard, S., et al. (2022). Environment-sensitivity functions for gross primary productivity in light use efficiency models. *Agricultural and Forest Meteorology*, *312*, 108708. https://doi.org/10.1016/j.agrformet.2021.108708

Bogena, H. R., Bol, R., Borchard, N., Brüggemann, N., Diekkrüger, B., Drüe, C., et al. (2015). A terrestrial observatory approach to the integrated investigation of the effects of deforestation on water, energy, and matter fluxes. *Science China Earth Sciences*, *57*, 1–6. https://doi.org/10.1007/s11430-014-4911-7

Bogena, H. R., Herbst, M., Huisman, J. A., Rodenbaum, U., Weuthen, A., & Vereecken, H. (2010). Potential of wireless sensor networks for measuring soil water content variability. *Vadose Zone Journal*, *9*(4), 1002–1013. https://doi.org/10.2136/vzj2009.0173

Bogena, H. R., Montzka, C., Huisman, J. A., Graf, A., Schmidt, M., Stockinger, M., et al. (2018). The TERENO-rur hydrological observatory, A multiscale multi-compartment research platform for the advancement of hydrological science. *Vadose Zone Journal*, *17*, 1–22. https://doi.org/10.2136/vzj2018.03.0055

Borchardt, H. (2012). *Einfluss periglazialer Deckschichten auf Abflusssteuerung am Beispiel des anthropogen überprägten Wüstebaches (Nationalpark Eifel)*. (Doctoral dissertation). RWTH Aachen University. Retrived from https://nbn-resolving.org/urn/resolver.pl?urn=urn:nbn:de:hbz:82-opus-45676

Breiman, L. (2001). Random forests. *Machine Learning*, *45*(1), 5–32. https://doi.org/10.1023/A:1010933404324

Brinkmann, N., Eugster, W., Zweifel, R., Buchmann, N., & Kahmen, A. (2016). Temperate tree species show identical response in tree water deficit but different sensitivities in sap flow to summer soil drying. *Tree Physiology*, *36*(12), 1508–1519. https://doi.org/10.1093/treephys/tpw062

Cabon, A., Kannenberg, A., Arain, A., Babst, F., Baldocchi, D., Belmecheri, S., et al. (2022). Cross-biome synthesis of source versus sink limits to tree growth. *Science*, *376*(6594), 758–761. https://doi.org/10.1126/science.abm4875

Canadell, J. G., Monteiro, P. M. S., Costa, M. H., Cotrim da Cunha, L., Cox, P. M., Eliseev, A. V., et al. (2021). Global carbon and other biogeochemical cycles and feedbacks. In *Climate change 2021, the physical science basis. Contribution of working group I to the sixth assessment report of the intergovernmental panel on climate change* (pp. 673–816). Cambridge University Press. https://doi.org/10.1017/9781009157896.007

Castro, S. M., Sanchez-Azofeifa, G. A., & Sato, H. (2018). Effect of drought on productivity in a Costa Rican tropical dry forest. *Environmental Research Letters*, *13*(4), 045001. https://doi.org/10.1088/1748-9326/aaacbc

Chen, T., & Guestrin, C. (2016). XGBoost, A scalable tree boosting system. In *Proceedings of the 22nd ACM SIGKDD international conference on knowledge discovery and data mining* (pp. 785–794). https://doi.org/10.48550/arXiv.1603.02754

Croft, H., Chen, J. M., Froelich, N. J., Chen, B., & Staebler, R. M. (2015). Seasonal controls of canopy chlorophyll content on forest carbon uptake: Implications for GPP modeling. *Journal of Geophysical Research: Biogeosciences*, *120*(8), 1576–1586. https://doi.org/10.1002/2015JG002980

Debeer, D., & Strobl, C. (2020). Conditional permutation importance revisited. *BMC Bioinformatics*, *21*(1), 307. https://doi.org/10.1186/s12859-020-03622-2

Dengel, S., Grace, J., & MacArthur, A. (2015). Transmissivity of solar radiation within a *Picea sitchensis* stand under various sky conditions. *Biogeosciences*, *12*(14), 4195–4207. https://doi.org/10.5194/bg-12-4195-2015

Denissen, J. M. C., Teuling, A. J., Pitman, A. J., Koirala, S., Migliavacca, M., Li, W., et al. (2022). Widespread shift from ecosystem energy to water limitation with climate change. *Nature Climate Change*, *12*(7), 677–684. https://doi.org/10.1038/s41558-022-01403-8

Doroszewski, A., Gorski, T., & Kozyra, J. (2015). Atmospheric moisture controls far-red irradiation, a probable impact on the phytochrome. *International Agrophysics*, *29*(3), 283–289. https://doi.org/10.1515/intag-2015-0033

Dusenge, M. E., Duarte, A. G., & Way, D. A. (2019). Plant carbon metabolism and climate change, elevated CO_2 and temperature impacts on photosynthesis, photorespiration and respiration. *New Phytologist*, *221*(1), 32–49. https://doi.org/10.1111/nph.15283

Ecomatik. (2005). *User manual for SF-L Sensor-Patent pendin*g. Version 1.3. (p. 9). Ecomatik Umweltmess-und Datentechnik.

Etmann, M. (2009). *Dendrologische Aufnahmen im Wassereinzugsgebiet Oberer Wüstebach anhand verschiedener Mess-und Schätzverfahren*. (Master thesis). University of Münster. Retrieved from JUSER https://juser.fz-juelich.de/record/10505

Ewers, B. E., Mackay, D. S., & Samanta, S. (2007). Interannual consistency in canopy stomatal conductance control of leaf water potential across seven tree species. *Tree Physiology*, *27*(1), 11–24. https://doi.org/10.1093/treephys/27.1.11

Farquhar, G. D., von Caemmerer, S., & Berry, J. A. (1980). A biochemical model of photosynthetic CO_2 assimilation in leaves of C_3 species. *Planta*, *149*(1), 78–90. https://doi.org/10.1007/BF00386231

Feng, C., Wang, H., Lu, N., Chen, T., He, H., Lu, Y., & Tu, X. M. (2014). Log-transformation and its implications for data analysis. *Shanghai Archives of Psychiatry*, *26*, 105–109. https://doi.org/10.3969/j.issn.1002-0829.2014.02.009

Friedman, J. H. (2002). Stochastic gradient boosting. *Computational Statistics & Data Analysis*, *38*(4), 367–378. https://doi.org/10.1016/S0167-9473(01)00065-2

Fu, Z., Ciais, P., Makowski, D., Bastos, A., Stoy, P. C., Ibrom, A., et al. (2021). Uncovering the critical soil moisture thresholds of plant water stress for European ecosystems. *Global Change Biology*, *28*(6), 2111–2123. https://doi.org/10.1111/gcb.16050

Garbulsky, M. F., Penuelas, J., Papale, D., Ardö, J., Goulden, M. L., Kiely, G., et al. (2010). Patterns and controls of the variability of radiation use efficiency and primary productivity across terrestrial ecosystems. *Global Ecology and Biogeography*, *19*(2), 253–267. https://doi.org/10.1111/j.1466-8238.2009.00504.x

Gitelson, A. A., & Gamon, J. A. (2015). The need for a common basis for defining light-use efficiency, Implications for productivity estimation. *Remote Sensing of Environment*, *156*, 196–201. https://doi.org/10.1016/j.rse.2014.09.017

Gitelson, A. A., Peng, Y., Arkebauer, T. J., & Schepers, J. (2014). Relationships between gross primary production, green LAI, and canopy chlorophyll content in maize, Implications for remote sensing of primary production. *Remote Sensing of Environment*, *144*, 65–72. https://doi.org/10.1016/j.rse.2014.01.004

Goldstein, G., Andrade, J. L., Meinzer, F. C., Holbrook, N. M., Cavelier, J., Jackson, P., & Celis, A. (1998). Stem water storage and diurnal patterns of water use in tropical forest canopy trees. *Plant, Cell & Environment*, *21*(4), 397–406. https://doi.org/10.1046/j.1365-3040.1998.00273.x

Goulden, M. L., Daube, B. C., Fan, S. M., Sutton, D. J., Bazzaz, A., Munger, J. W., & Wofsy, S. C. (1997). Physiological responses of a black spruce forest to weather. *Journal of Geophysical Research*, *102*(D24), 28987–28996. https://doi.org/10.1029/97JD01111

Graf, A., Bogena, H. R., Drüe, C., Hardelauf, H., Pütz, T., Heinemann, G., & Vereecken, H. (2014). Spatiotemporal relations between water budget components and soil water content in a forested tributary catchment. *Water Resources Research*, *50*(6), 4837–4857. https://doi.org/10.1002/2013WR014516

Granier, A. (1987). Evaluation of transpiration in a Douglas-fir stand by means of sap flow measurements. *Tree Physiology*, *3*(4), 309–320. https://doi.org/10.1093/treephys/3.4.309

Green, D. S., Erickson, J. E., & Kruger, E. L. (2003). Foliar morphology and canopy nitrogen as predictors of light-use efficiency in terrestrial vegetation. *Agricultural and Forest Meteorology*, *115*(3–4), 163–171. https://doi.org/10.1016/S0168-1923(02)00210-1

Grömping, U. (2009). Variable importance assessment in regression, linear regression versus random forest. *The American Statistician*, *63*(4), 308–319. https://doi.org/10.1198/tast.2009.08199

Hedges, L. V., Gurevitch, J., & Curtis, P. S. (1999). The meta-analysis of response ratios in experimental ecology. *Ecology*, *80*(4), 1150–1156. https://doi.org/10.1890/0012-9658(1999)080[1150:TMAORR]2.0.CO;2

Heraut-Bron, V., Robin, C., Varlet-Grancher, C., Afif, D., & Guckert, A. (2000). Light quality (red: Far-red ratio), does it affect photosynthetic activity, net CO_2 assimilation, and morphology of young white clover leaves? *Canadian Journal of Botany*, *77*(10), 1425–1431. https://doi.org/10.1139/b99-099

Hertel, C., Leuchner, M., & Menzel, A. (2011). Vertical variability of spectral ratios in a mature mixed forest stand. *Agricultural and Forest Meteorology*, *151*(8), 1096–1105. https://doi.org/10.1016/j.agrformet.2011.03.013

Horn, J. E., & Schulz, K. (2011). Identification of a general light use efficiency model for gross primary production. *Biogeosciences*, *8*(4), 999–1021. https://doi.org/10.5194/bg-8-999-2011

Hothorn, T., Hornik, K., & Zeileis, A. (2006). Unbiased recursive partitioning: A conditional inference framework. *Journal of Computational and Graphical Statistics*, *15*(3), 651–674. https://doi.org/10.1198/106186006X133933

Kalliokoski, T., Mäkelä, A., Fronzek, S., Minunno, F., & Peltoniemi, M. (2018). Decomposing sources of uncertainty in climate change projections of boreal forest primary production. *Agricultural and Forest Meteorology*, *262*, 192–205. https://doi.org/10.1016/j.agrformet.2018.06.030

Katul, G., Leuning, R., & Oren, R. (2003). Relationship between plant hydraulic and biochemical properties derived from a steady-state coupled water and carbon transport model. *Plant, Cell & Environment*, *26*(3), 339–350. https://doi.org/10.1046/j.1365-3040.2003.00965.x

Keenan, T. F., Baker, I., Barr, A., Ciais, P., Davis, K., Dietze, M., et al. (2012). Terrestrial biosphere model performance for inter-annual variability of land-atmosphere CO_2 exchange. *Global Change Biology*, *18*(6), 1971–1987. https://doi.org/10.1111/j.1365-2486.2012.02678.x

Klein, T., Rotenberg, E., Tatarinov, F., & Yakir, D. (2016). Association between sap flow-derived and eddy covariance-derived measurements of forest canopy CO_2 uptake. *New Phytologist*, *209*(1), 436–446. https://doi.org/10.1111/nph.13597

Kormann, R., & Meixner, F. X. (2001). An analytical footprint model for non-neutral stratification. *Boundary-Layer Meteorology*, *99*(2), 207–224. https://doi.org/10.1023/A:1018991015119

Köstner, B., Granier, A., & Cermak, J. (1998). Sapflow measurements in forest stands, methods and uncertainties. *Annals of Forest Science*, *55*(1–2), 13–27. https://doi.org/10.1051/forest:19980102

Kotilainen, T., Aphalo, P. J., Brelsford, C. C., Böök, H., Devraj, S., Heikkilä, A., et al. (2020). Patterns in the spectral composition of sunlight and biologically meaningful spectral photon ratios as affected by atmospheric factors. *Agricultural and Forest Meteorology*, *291*, 108041. https://doi.org/10.1016/j.agrformet.2020.108041

Kuhn, M. (2008). Building predictive models in R using the caret package. *Journal of Statistical Software*, *28*(5), 1–26. https://doi.org/10.18637/jss.v028.i05

Kulmala, L., Pumpanen, J., Kolari, P., MuukkonenHari, P., & Vesala, T. (2011). Photosynthetic production of ground vegetation in different-aged Scots pine (*Pinus sylvestris*) forests. *Canadian Journal of Forest Research*, *41*(10), 2020–2030. https://doi.org/10.1139/x11-121

Lange, M., Dechant, B., Rebmann, C., Vohland, M., Cuntz, M., & Doktor, D. (2017). Validating MODIS and sentinel-2 NDVI products at a temperate deciduous forest site using two independent ground-based sensors. *Sensors*, *17*(8), 1855. https://doi.org/10.3390/s17081855

Law, B. E., Falge, E., Gu, L., Baldocchi, D. D., Bakwin, P., Berbigier, P., et al. (2002). Environmental controls over carbon dioxide and water vapor exchange of terrestrial vegetation. *Agricultural and Forest Meteorology*, *113*(1–4), 97–120. https://doi.org/10.1016/S0168-1923(02)00104-1

Leuchner, M., Hertel, C., & Menzel, A. (2011). Spatial variability of photosynthetically active radiation in European beech and Norway spruce. *Agricultural and Forest Meteorology*, *151*(9), 1226–1232. https://doi.org/10.1016/j.agrformet.2011.04.014

Li, W., Yu, T. F., Li, X. Y., & Zhao, C. Y. (2016). Sap flow characteristics and their response to environmental variables in a desert riparian forest along lower Heihe River Basin, Northwest China. *Environmental Monitoring and Assessment*, *188*(10), 561. https://doi.org/10.1007/s10661-016-5570-2

Liu, Y., & Just, A. (2021). SHAPforxgboost, SHAP plots for 'XGBoost'. R package version 0.1.1.

Long, S. P. (1991). Modification of the response of photosynthetic productivity to rising temperature by atmospheric CO_2 concentrations: Has its importance been underestimated? *Plant, Cell & Environment*, *14*(8), 729–739. https://doi.org/10.1111/j.1365-3040.1991.tb01439.x

Lundberg, S. M., & Lee, S. I. (2017). A unified approach to interpreting model predictions. *Advances in Neural Information Processing Systems*, *30*, 4768–4777. https://doi.org/10.48550/arXiv.1705.07874

Mäkelä, A., Pulkkinen, M., Kolari, P., Lagergren, F., Berbigier, P., Lindroth, A., et al. (2008). Developing an empirical model of stand GPP with the LUE approach, analysis of eddy covariance data at five contrasting conifer sites in Europe. *Global Change Biology*, *14*(1), 92–108. https://doi.org/10.1111/j.1365-2486.2007.01463.x

Martini, D., Sakowska, K., Wohlfahrt, G., Pacheco-Labrador, J., van der Tol, C., Porcar-Castell, A., et al. (2022). Heatwave breaks down the linearity between sun-induced fluorescence and gross primary production. *New Phytologist*, *233*(6), 2415–2428. https://doi.org/10.1111/nph.17920

Mauder, M., Cuntz, C., Drüe, C., Graf, A., Rebmann, C., Schmid, H. P., et al. (2013). A strategy for quality and uncertainty assessment of long-term eddy-covariance measurements. *Agricultural and Forest Meteorology*, *169*, 122–135. https://doi.org/10.1016/j.agrformet.2012.09.006

Mauder, M., & Foken, T. (2011). *Documentation and instruction manual of the eddy-covariance software package TK3*. Universität Bayreth, Abteilung Mikrometeorologie. Arbeitsergebnisse, (Vol. 46).

Montagnani, L., Grünwald, T., Kowalski, A., Mammarella, I., Merbold, L., Metzger, S., et al. (2018). Estimating the storage term in eddy covariance measurements, the ICOS methodology. *International Agrophysics*, *32*(4), 551–567. https://doi.org/10.1515/intag-2017-0037

Monteith, J. L. (1972). Solar radiation and productivity in tropical ecosystems. *Journal of Applied Ecology*, *9*(3), 747–766. https://doi.org/10.2307/2401901

Motzer, T., Munz, N., Küppers, M., Schmitt, D., & Anhuf, D. (2005). Stomatal conductance, transpiration and sap flow of tropical montane rain forest trees in the southern Ecuadorian Andes. *Tree Physiology*, *25*(10), 1283–1293. https://doi.org/10.1093/treephys/25.10.1283

Nestola, E., Calfapietra, C., Emmerton, C. A., Wong, C. Y. S., Thayer, D. R., & Gamon, J. A. (2016). Monitoring grassland seasonal carbon dynamics, by integrating MODIS NDVI, proximal optical sampling, and eddy covariance measurements. *Remote Sensing*, *8*(3), 260. https://doi.org/10.3390/rs8030260

Neuwirth, B., Rabbel, I., Bendix, J., Bogena, H. R., & Thies, B. (2021). The European heat wave 2018, the dendroecological response of oak and spruce in western Germany. *Forests*, *12*(3), 283. https://doi.org/10.3390/f12030283

O'Brien, J. J., Oberbauer, S. F., & Clark, D. B. (2004). Whole tree xylem sap flow responses to multiple environmental variables in a wet tropical forest. *Plant, Cell & Environment*, *27*(5), 551–567. https://doi.org/10.1111/j.1365-3040.2003.01160.x

Pan, Y., Birdsey, R. A., Fang, Y., Houghton, R., Kauppi, P. E., Kurz, W. A., et al. (2011). A large and persistent carbon sink in the world's forests. *Science*, *333*(6045), 988–993. https://doi.org/10.1126/science.1201609

Peltola, O., Lapo, K., & Thomas, C. K. (2021). A physics-based universal indicator for vertical decoupling and mixing across canopies architectures and dynamic stabilities. *Geophysical Research Letters*, *48*(5), e2020GL091615. https://doi.org/10.1029/2020GL091615

Peng, Y., Gitelson, A. A., Keydan, G., Rundquist, D. C., & Moses, W. (2011). Remote estimation of gross primary production in maize and support for a new paradigm based on total crop chlorophyll content. *Remote Sensing of Environment*, *115*(4), 978–989. https://doi.org/10.1016/j.rse.2010.12.001

Perämäki, M., Vesala, T., & Nikinmaa, E. (2005). Modeling the dynamics of pressure propagation and diameter variation in tree sapwood. *Tree Physiology*, *25*(9), 1091–1099. https://doi.org/10.1093/treephys/25.9.1091

Putzenlechner, B., Castro, S., Kiese, R., Ludwig, R., Marzahn, P., Sharp, I., & Sanchez-Azofeifa, A. (2019). Validation of Sentinel-2 fAPAR products using ground observations across three forest ecosystems. *Remote Sensing of Environment*, *232*, 111310. https://doi.org/10.1016/j.rse.2019.111310

Putzenlechner, B., Marzahn, P., Kiese, R., Ludwig, R., & Sanchez-Azofeifa, A. (2019). Assessing the variability and uncertainty of two-flux FAPAR measurements in a conifer-dominated forest. *Agricultural and Forest Meteorology*, *264*, 149–163. https://doi.org/10.1016/j.agrformet.2018.10.007

Putzenlechner, B., Marzahn, P., & Sanchez-Azofeifa, A. (2020). Accuracy assessment on the number of flux terms needed to estimate in situ fAPAR. *International Journal of Applied Earth Observation and Geoinformation*, *88*, 102061. https://doi.org/10.1016/j.jag.2020.102061

Raj, R., Hamm, N. A. S., van der Tol, C., & Stein, A. (2016). Uncertainty analysis of gross primary production partitioned from net ecosystem exchange measurements. *Biogeosciences*, *13*(5), 1409–1422. https://doi.org/10.5194/bg-13-1409-2016

Ranghetti, L., Boschetti, M., Nutini, F., & Busetto, L. (2020). "sen2r", an R toolbox for automatically downloading and preprocessing Sentinel-2 satellite data. *Computers & Geosciences*, *139*, 104473. https://doi.org/10.1016/j.cageo.2020.104473

Reichstein, M., Falge, E., Baldocchi, D., Papale, D., Aubinet, M., Berbigier, P., et al. (2005). On the separation of net ecosystem exchange into assimilation and ecosystem respiration: Review and improved algorithm. *Global Change Biology*, *11*(9), 1424–1439. https://doi.org/10.1111/j.1365-2486.2005.001002.x

Roddy, A. B., & Dawson, T. (2013). Novel patterns of hysteresis in the response of leaf-level sap flow to vapor pressure deficit. *Acta Horticulturae*, *991*, 261–267. https://doi.org/10.17660/ActaHortic.2013.991.32

Running, S. W., & Zhao, M. (2015). Daily GPP and annual NPP (MOD17A2/A3) products NASA Earth Observing System MODIS land algorithm. In *MOD17 User's Guide*. MODIS Land Team.

Steppe, K., Vandegehuchte, M. W., Tognetti, R., & Mencuccini, M. (2015). Sap flow as a key trait in the understanding of plant hydraulic functioning. *Tree Physiology*, *35*(4), 341–345. https://doi.org/10.1093/treephys/tpv033

Stocker, B. D., Wang, H., Smith, N. G., Harrison, S. P., Keenan, T. F., Sandroval, D., et al. (2020). P-model v1.0, an optimality-based light use efficiency model for simulating ecosystem gross primary production. *Geoscientific Model Development*, *13*(3), 545–1581. https://doi.org/10.5194/gmd-13-1545-2020

Strobl, C., Boulesteix, A. L., Kneib, T., Augustin, T., & Zeileis, A. (2008). Conditional variable importance for random forests. *BMC Bioinformatics*, *9*(1), 307. https://doi.org/10.1186/1471-2105-9-307

Tao, X., Liang, S., & Wang, D. (2015). Assessment of five global satellite products of fraction of absorbed photosynthetically active radiation: Intercomparison and direct validation against ground-based data. *Remote Sensing of Environment*, *163*, 270–285. https://doi.org/10.1016/j.rse.2015.03.025

Taye, F. A., Folkersen, M. V., Fleming, C. M., Buckwell, A., Mackay, B., Diwakar, K. C., et al. (2021). The economic values of global forest ecosystem services: A meta-analysis. *Ecological Economics*, *189*, 107145. https://doi.org/10.1016/j.ecolecon.2021.107145

Tuller, M., & Or, D. (2004). Water retention and characteristic curve. In D. Hillel (Ed.), *Encyclopedia of soils in the environment*. Elsevier Ltd.

Turnbull, M. H. (1991). The effect of light quantity and quality during development on the photosynthetic characteristics of six Australian rainforest tree species. *Oecologia*, *87*(1), 110–117. https://doi.org/10.1007/BF00323788

Urban, O., Janous, D., Acosta, M., Czerny, R., Markova, I., Navratil, M., et al. (2007). Ecophysiological controls over the net ecosystem exchange of mountain spruce stand. Comparison of the response in direct vs. diffuse solar radiation. *Global Change Biology*, *13*(1), 157–168. https://doi.org/10.1111/j.1365-2486.2006.01265.x

Urban, O., Klem, K., Ac, A., Havrankova, K., Holisova, P., Navratil, M., et al. (2012). Impact of clear and cloudy sky conditions on the vertical distribution of photosynthetic CO_2 uptake within a spruce canopy. *Functional Ecology*, *26*(1), 46–55. https://doi.org/10.1111/j.1365-2435.2011.01934.x

Vesala, T., Markkanen, T., Palva, L., Siivola, E., Palmroth, S., & Hari, P. (2000). Effect of variations of PAR on CO_2 exchange estimation for Scots pine. *Agricultural and Forest Meteorology*, *100*(4), 337–347. https://doi.org/10.1016/S0168-1923(99)00146-X

Wang, H., Tetzlaff, D., & Soulsby, C. (2019). Hysteretic response of sap flow in Scots pine (*Pinus sylvestris*) to meteorological forcing in a humid low-energy headwater catchment. *Ecohydrology*, *12*(6), e2125. https://doi.org/10.1002/eco.2125

Wang, S., Ibrom, A., Bauer-Gottwein, P., & Garcia, M. (2018). Incorporating diffuse radiation into a light use efficiency and evapotranspiration model, an 11-year study in a high latitude deciduous forest. *Agricultural and Forest Meteorology*, *248*, 479–493. https://doi.org/10.1016/j.agrformet.2017.10.023

Wang, Y., Zeng, Y., Yu, L., Yang, P., Van der Tol, C., Yu, Q., et al. (2021). Integrated modeling of canopy photosynthesis, fluorescence, and the transfer of energy, mass, and momentum in the soil–plant–atmosphere continuum (STEMMUS–SCOPE v1.0.0). *Geoscientific Model Development*, *14*(3), 379–1407. https://doi.org/10.5194/gmd-14-1379-2021

Weiss, M., Baret, F., & Jay, S. (2020). S2ToolBox Level 2 products, LAI, FAPAR, FCOVER. V2.0.

Widlowski, J. L. (2010). On the bias of instantaneous FAPAR estimates in open-canopy forests. *Agricultural and Forest Meteorology*, *150*(12), 1501–1522. https://doi.org/10.1016/j.agrformet.2010.07.011

Wieneke, S., Burkart, A., Cendrero-Mateo, M. P., Julitta, T., Rossini, M., Schickling, A., et al. (2018). Linking photosynthesis and sun-induced fluorescence at sub-daily to seasonal scales. *Remote Sensing of Environment*, *219*, 247–258. https://doi.org/10.1016/j.rse.2018.10.019

Williams, M., Rastetter, E. B., Van der Pol, L., & Shaver, G. R. (2014). Arctic canopy photosynthetic efficiency enhanced under diffuse light, linked to a reduction in the fraction of the canopy in deep shade. *New Phytologist*, *202*(4), 1266–1276. https://doi.org/10.1111/nph.12750

Williamson, B. D., Gilbert, P. B., Carone, M., & Simon, N. (2021). Nonparametric variable importance assessment using machine learning techniques. *Biometrics*, *77*(1), 9–22. https://doi.org/10.1111/biom.13392

Wu, G., Jiang, C., Kimm, H., Wang, S., Bernacchi, C., Moore, C. E., et al. (2022). Difference in seasonal peak timing of soybean far-red SIF and GPP explained by canopy structure and chlorophyll content. *Remote Sensing of Environment*, *279*, 113104. https://doi.org/10.1016/j.rse.2022.113104

Wutzler, T., Lucas-Moffat, A., Migliavacca, M., Knauer, J., Sickel, K., Sigut, L., et al. (2018). Basic and extensible post-processing of eddy covariance flux data with REddyProc. *Biogeosciences*, *15*(16), 5015–5030. https://doi.org/10.5194/bg-15-5015-2018

Xiao, X., Hollinger, D., Aber, J., Goltz, M., Davidson, E. A., Zhang, Q., & Moore, B., III. (2004). Satellite-based modeling of gross primary production in an evergreen needleleaf forest. *Remote Sensing of Environment*, *89*(4), 519–534. https://doi.org/10.1016/j.rse.2003.11.008

Xu, Z., Wu, Z., He, H., Guo, X., & Zhang, Y. (2021). Comparison of soil moisture at different depths for drought monitoring based on improved soil moisture anomaly percentage index. *Water Science and Engineering*, *14*(3), 171–183. https://doi.org/10.1016/j.wse.2021.08.008

Zeppel, M. J. B., Murray, B. R., Barton, C., & Eamus, D. (2004). Seasonal responses of xylem sap velocity to VPD and solar radiation during drought in a stand of native trees in temperate Australia. *Functional Plant Biology*, *31*(5), 461–470. https://doi.org/10.1071/FP03220

Zha, T., Qian, D., Jia, X., Bai, Y., Tian, Y., Bourque, C. P. A., et al. (2017). Soil moisture control of sap-flow response to biophysical factors in a desert-shrub species, *Artemisia ordosica*. *Biogeosciences*, *14*(19), 4533–4544. https://doi.org/10.5194/bg-14-4533-2017

Zhang, Q., Manzoni, S., Katul, G., Porporato, A., & Yang, D. (2014). The hysteretic evapotranspiration—Vapor pressure deficit relation. *Journal of Geophysical research: Biogeosciences*, *119*(2), 125–140. https://doi.org/10.1002/2013JG002484

Zhen, S., & Bugbee, B. (2020). Far-red photons have equivalent efficiency to traditional photosynthetic photons, Implications for redefining photosynthetically active radiation. *Plant, Cell & Environment*, *43*(5), 1259–1272. https://doi.org/10.1111/pce.13730

References From the Supporting Information

Hastie, T. J., & Tibshirani, R. J. (1990). *Generalized additive models*. Chapman and Hall.